CONGENITAL
CARDIOLOGY TODAY

Timely News and Information for BC/BE Congenital/Structural Cardiologists and Surgeons

Fluid Viscosity Increases Pressure Drop and Exacerbates Flow-Energy Loss (Relevance to Modified-Fontan Patients with Elevated Hematocrit)

By Robert Ascuitto PhD, MD; Nancy Ross-Ascuitto MD; Martin Guillot, PhD

Abstract

In the Fontan circulation, cavopulmonary obstructions can create flow disturbances conducive to energy dissipation. We postulated an elevated hematocrit would worsen such flow-energy wastage through its increase in blood viscosity (η). Computer modeling of a viscous fluid flowing through a conduit was taken to simulate blood traversing a portion of a Fontan cavopulmonary pathway. A tubular conduit was assumed to undergo an abrupt decrease ($A{\rightarrow}a$) or increase ($a{\rightarrow}A$) in cross-sectional area (A, a), for flow transitions involving with ($a = A/2$) or ($a = A/4$). Viscosity values, [(3-8) x 10^{-3}kg/m-s], were determined from clinically relevant blood hematocrits, (30% – 70%). Flow rate was fixed at 1.67×10^{-5} m^3/s (1.0 L/min). Numerical solutions (finite volume analysis) to the Navier-Stokes equations were used to calculate pressure drops [$\Delta P(\eta)$] and flow-energy losses [$\Delta E (\eta)$]. Our findings demonstrate $\Delta P(\eta)$ and $\Delta E (\eta)$ increase markedly with increasing viscosity, and with hematocrit. For flow contraction ($A{\rightarrow}a$), $\Delta P(\eta)$ ranged from [71.94 N/m^2 (0.54 mmHg) to 110.62 N/m^2 (0.83 mmHg)] and [352.36 N/m^2 (2.66 mmHg) to 496.30 N/m^2 (3.74 mmHg)], and $\Delta E (\eta)$ [22.46 N/m^2 (0.17 mmHg) to 52.85 N/m^2 (0.40 mmHg)] and [94.95 N/m^2 (0.72 mmHg) to 201.80 N/m^2 (1.52 mmHg)]; for ($a = A/2$) and ($a=A/4$), respectively. For flow expansion ($a{\rightarrow}A$), $\Delta P (\eta)$ ranged from [3.41 N/m^2 (0.03 mmHg) to 17.36 N/m^2 (0.13 mmHg)] and [47.24 N/m^2 (0.37 mmHg) to 120.98 N/m^2 (0.91 mmHg)], and $\Delta E (\eta)$ [23.29 N/m^2 (0.18 mmHg) to 56.45 N/m^2 (0.43 mmHg)] and [87.73 N/m^2 (0.66 mmHg) to 221.70 N/m^2 (1.67 mmHg)]; for ($a=A/2$) and ($a=A/4$), respectively. Thus, fluid viscosity worsens pressure gradients and exacerbates flow-energy losses. These findings have important clinical implications for pulmonary artery (and systemic venous) pressure, effective lung perfusion and efficient long-term cardiac performance in Fontan patients with cavopulmonary obstruction and elevated hematocrit from chronic hypoxemia.

Introduction

The Fontan procedure with its various modifications (currently the Total Cavopulmonary Connection) has become the surgical palliation of choice for patients with functional single-ventricle heart disease[1-4]. The operations entail channeling systemic venous return from the superior vena cava and inferior vena cava directly to the pulmonary arteries. Thus, following Fontan completion, an important factor governing successful hemodynamic performance is the capacity of the surgically-crafted cavopulmonary pathway to conserve the traversing blood flow's mechanical energy, i.e. energy available for flow propagation. Energy loss arises from anatomical and/or functional obstruction to flow[5-7]. Anatomical obstruction can be caused by an

---

CONGENITAL CARDIOLOGY TODAY

Call for Cases and Other Original Articles

Do you have interesting research results, observations, human interest stories, reports of meetings, etc. to share?
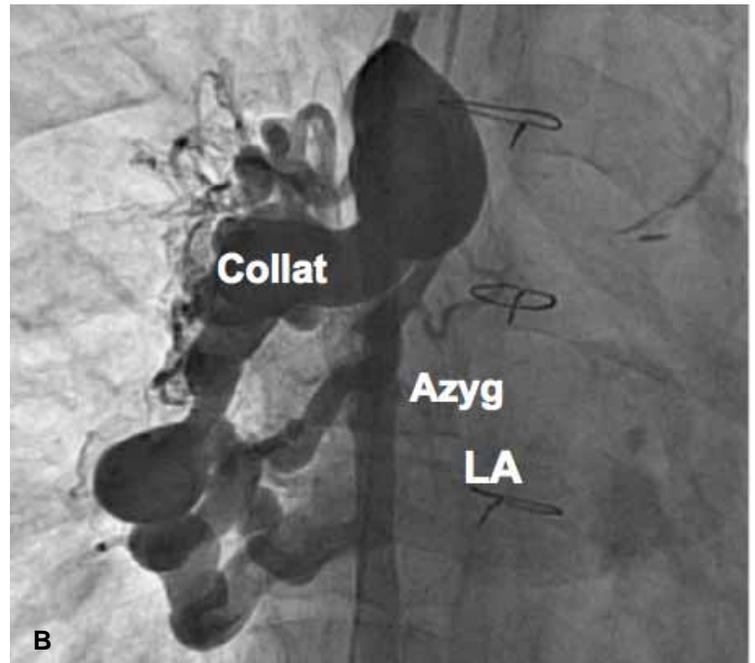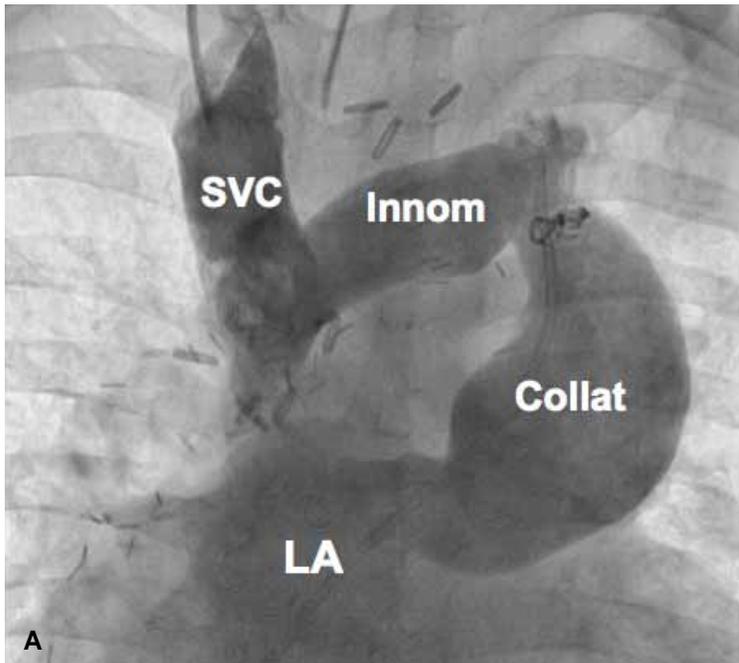Submit your manuscript to: RichardK@CCT.bz

Figure 1: A. *Angiography of the right superior vena cava (SVC) in a patient with hypoplastic left heart syndrome (HPLH) after stage I (Norwood operation), stage II (bidirectional Glenn shunt) and stage III (completion of Fontan procedure-extra cardiac inferior vena cava to right pulmonary artery conduit). Contrast shows retrograde filling of the SVC and the innominate (Innom) vein. A large bulbous venous collateral (Collat) - levo-atrial cardinal vein - connects the Innom vein to the left atrium (LA), resulting in a large right-to-left shunt. The venous collateral provided a pathway of lesser resistance compared to the left pulmonary artery, insomuch as the left pulmonary artery had proximal narrowing (not seen in this frame). The patient presented with hematocrit 60%. A vascular stent was placed in the proximal left pulmonary artery and two large vascular plugs were used to occlude the venous collateral. The authors wish to thank Dr. Albert Gutierrez for referring this patient for treatment.*
B. *Angiography of the right superior vena cava (SVC) in a patient with (HPLH) after stage I, II and III, as described in (A) above. Contrast shows retrograde filling of the right SVC and azygous (Azyg) vein. A large plexus of venous collaterals (Collat) connects the Azyg vein to the left atrium (LA). The patient presented with hematocrit 60%. Several large coils were used to occlude the venous collaterals.*

abrupt change in cross-sectional area of a vessel or conduit. In contrast, functional obstruction is related to the viscosity (internal friction) associated with a fluid (blood) in motion.

Modified-Fontan patients are at risk of developing progressive right-to-left shunting of blood through: a surgically-created fenestration in the inferior vena cava-to-right pulmonary artery conduit, systemic venous baffle leaks, systemic venous-to-atrial/pulmonary venous collateral vessels (Figure 1) and pulmonary arteriovenous fistulae. These shunts often become more pronounced with ventricular dysfunction. Each shunt contributes to decompressing the cavopulmonary pathway, at the expense of systemic arterial desaturation. However, a sustained decrease in arterial oxygen tension ultimately leads to an erythrocytosis with a concomitant increase in hematocrit, an important determinant of blood viscosity. Viscosity originates with cohesive interactions among cells and proteins, which oppose the flow of blood. Thus, as the percentage of red blood cells in plasma rises, the disproportionate increase in viscosity would be expected to worsen flow-energy losses across cavopulmonary obstructions, and thereby further reduce efficiency of a Fontan circulation.

Therefore, the purpose of this investigation was to assess effects of viscosity on pressure drop and energy loss associated with flow undergoing a sudden contraction or expansion, as would be required for flow to enter or leave a region of pathway narrowing. A computational fluid dynamics (CFD) analysis of non-pulsatile (passive) fluid flow through a conduit was taken to simulate blood crossing a portion of a Fontan cavopulmonary pathway. Viscosity values were chosen to reflect clinically-relevant blood hematocrits. Pressure distributions and flow-velocity fields were constructed from numerical solutions (finite volume analysis) to the fluid-flow (Navier-Stokes) equations describing the proposed flow transitions. Since viscosity represents a dissipative process, an increasing value should manifest itself through further attenuation of pressure and velocity in the direction of flow. Thus, we postulated as viscosity of the moving fluid becomes greater, there would be a corresponding increase in pressure drop and an exacerbation of flow-energy loss associated with a localized region of pathway narrowing.

Materials and Methods

Model Description

Non-pulsatile, incompressible, viscous-fluid flowing through a vessel or conduit was taken to satisfy the mechanical-energy balance equations:

$$\Delta P_{i,f} = (<P>_i - <P>_f) \qquad (1a)$$
$$\Delta P_{i,f} = (<K>_f - <K>_i) + \Delta E_{i,f}. \qquad (1b)$$

The terms <P> and <K> represent "flow-averaged" pressure (P) and "flow-averaged" kinetic energy (K), respectively. The quantity $\Delta E_{i,f}$ denotes the energy loss per unit of fluid volume. The subscripts (i) and (f) designate the initial (i) position for unperturbed (incoming) and the final (f) position for downstream (outgoing), fluid flow. The various terms, and the flow-averaging procedures, are defined in the Appendix. Equations (1) describe the overall pressure change ($\Delta P_{i, f}$) associated with the fluid transition (i→ f), in terms of the flow's:

1) change in kinetic energy ($\Delta K_{f,i} = <K>_f - <K>_i$) due to the alteration in vessel cross-sectional area, and

2) energy loss ($\Delta E_{i,f}$) arising as a consequence of viscous dissipation. The quantities $\Delta P_{i, f}$, $\Delta K_{f,i}$ and $\Delta E_{i,f}$ depend on fluid viscosity and flow rate. Each of these quantities represents energy per unit of fluid volume and thus carries dimensions of pressure. The deformation of the vessel or conduit was considered to be so small that work done by forces (shear and normal stresses) acting on the wall would be negligible. Numerical solutions to the fluid-flow (Navier - Stokes) equations were used to construct (map) pressure distributions and flow velocity fields from which $\Delta P_{i,f}$ and $\Delta E_{i,f}$ were calculated. We have assumed the fluid to be of Newtonian character, a generally valid approximation for the behavior of blood flow in larger vessels.

Model Parameters

Pressure drop and flow-energy loss as a function of fluid viscosity were assessed for flow encountering a sudden decrease (Figure 2A) or increase (Figure 2B) in vessel cross-sectional area. This arrangement was used to simulate flow entering or leaving a region of vessel narrowing. These fluid pathways combine geometric simplicity with complex flow behavior relevant to Fontan cavopulmonary anatomy. We considered two types of obstructions: 1) relatively mild, a = A/2 (or d = 0.7 D) and 2) more severe, a = A/4 (or d = 0.5 D), where A(a) represent the cross-sectional areas and D(d) the corresponding diameters of the vessels (see Figure 2). The fluid pathway was taken to have an overall length of 0.07 m and an unobstructed diameter (D) of 0.012 m.

Viscosity values were based on data collected from in-vitro experiments relating viscosity to hematocrit, for whole blood (8-10), in conjunction with hemodynamic calculations. The calculations entailed estimating shear rate, an important determinate of fluid viscosity, for blood flowing through a non-obstructed portion of a Fontan cavopulmonary pathway. Assuming steady (Poiseuille) flow, shear rate is $8V_{avg}/D$, where V_{avg} is average flow velocity and D vessel diameter. Taking V_{avg} to be typical for cavopulmonary blood flow (~0.2 m/s) and a D of 0.012 m (as in our model), shear rate becomes ~130 s^{-1}. Wells and Merrill determined in-vitro viscosity – hematocrit relationships for a variety of measured shear rates[9]. Based on these investigators' findings and our calculated shear rate, viscosity values would range from (3–8)X10^{-3} kg/m-s for hematocrits of (30%-70%). (The viscosity of plasma (37°C) is ~1.8 X10^{-3} kg/m-s.). Figure 3 shows curves relating viscosity to hematocrit. For simplicity, relative viscosity (3 – 8)- (relative to the viscosity of water, 1X10^{-3} kg/m-s) - was used in the figures. Fluid density was taken as 1050 kg/m^3. A typical flow rate of 1.67 X 10^{-5} m^3/s (1.0 L/min) was used. The quantities $\Delta P_{i,f}$ (η) and $\Delta E_{i,f}$ (η) were plotted against relative viscosity (η), and against corresponding hematocrit. When constructing graphs for $\Delta P_{i, f}$ (η) and $\Delta E_{i, f}$ (η) vs. hematocrit, the fluid-flow equations were solved using the mean values of viscosity corresponding to the desired hematocrits (see Figure 3). The mean value of viscosity was found to increase exponentially with respect to hematocrit.

Numerical Analysis

Flow simulation studies were performed using the commercial CFD software package Fluent 12.1 (Ansys, Inc., Lebanon, NH). For the fluid pathways considered, flow symmetry about the centerline was exploited so that the two-dimensional axially-symmetric fluid flow (Navier-Stokes) equations could be solved, rather than their three-dimensional counterparts. This simplification considerably reduces the computational effort required to achieve convergent numerical solutions.

Mesh Generation

Finite volume analysis was used to numerically solve the Navier-Stokes equations. This procedure involves dividing the computational domain into a number of contiguous elements, called cells. Meshes, which are required for the numerical analysis, were constructed (like a spider web) over the computational domain. They were generated using a CFD software program (Ansys, Inc, Lebanon, NH). "Coarse" and "fine" meshes were utilized for each of the cases studied (relatively mild/more severe and flow contraction/flow expansion), the

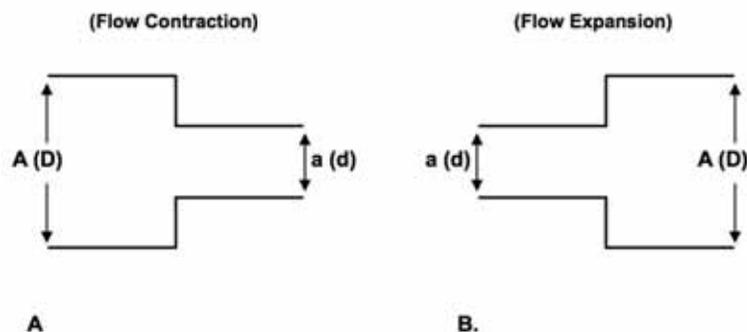*Figure 2: Flow Pathways - Schematic representation of the tubular fluid pathways considered. A. A sudden decrease in vessel cross-sectional area, taken to characterize flow contracting as it enters a region of vessel narrowing. B. A sudden increase in vessel cross-sectional area, taken to characterize flow expanding as it leaves a region of vessel narrowing. A (a) represent the cross-sectional areas and D (d) the corresponding diameters of the vessels, A (D) > a (d).*

CFD analysis was performed with both types of meshes to ensure numerical solutions were independent of mesh size. Larger cells were located upstream of the change in cross-sectional area near the centerline of the vessel, where flow does not exhibit rapid spatial variation. Smaller cells were placed near the vessel walls and downstream from the obstruction, to resolve flow characteristics associated with wall shear stresses and more complex flow behavior (such as vortices, flow reversal, etc.) arising as the outgoing fluid equilibrates.

Boundary Conditions

Solutions to the Navier-Stokes equations require imposing boundary conditions on the computational domain. For the geometries considered, boundary conditions are required at the flow inlet, vessel wall and flow outlet. The Reynolds number for inlet flow,
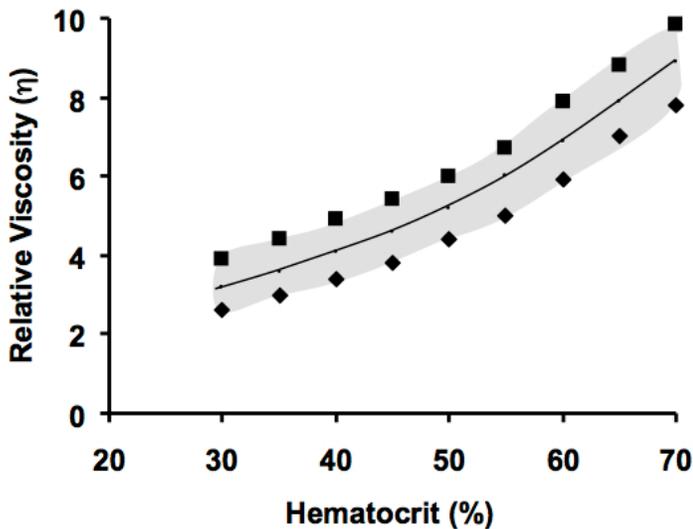
Figure 3: Relative Viscosity vs. Hematocrit - Relative viscosity (η), unitless, is on the y-axis and hematocrit (%) on the x-axis. Relative viscosity is defined as absolute viscosity, in kg/m-s, divided by the viscosity of water, 1 x 10⁻³ kg/m-s.
The upper curve (■) provides an upper limit for the viscosity – hematocrit curve. The lower curve (♦) provides a lower limit for the viscosity – hematocrit curve. Curves are based on data obtained from in-vitro experiments using whole blood (8-10). The solid curve represents mean values of viscosity as a function of hematocrit. The exponential regression line for the mean values of viscosity is $y = 1.42e^{0.026x}$ ($R^2 = 0.99$).

$Re_D = \rho V_{avg} D/\eta$, ranged from 328 to 619, consistent with laminar flow. The incoming fluid stream exhibited fully developed flow (parabolic velocity profiles) prior to encountering the decrease or increase in the vessel cross-sectional area. The parabolic velocity profiles specified at the inlet were such that V_{avg} multiplied by the cross-sectional area (A or a) yielded the desired flow rate. The "no-slip" boundary condition (zero velocity) was imposed at the vessel wall. The downstream pressure at the end of the fluid pathway was fixed at 1591 N/m² (12 mmHg), typical of Fontan pulmonary arterial pressure.

Results

The fluid transitions were characterized by either an abrupt decrease (flow contraction) or a sudden increase (flow expansion) in vessel cross-sectional area (Figure 2). A relatively mild, a=A/2 (or d=0.7 D), and a more severe, a=A/4 (or d=0.5 D), form of flow obstruction were considered (see Materials and Methods).

I. Flow Contraction (Figure 2A)

Flow-averaged pressure drop, $\Delta P_{i,f}$ (η), from the left-hand side of Eq (1a), increased uniformly as viscosity (Figure 4A), and hematocrit (Figure 4B), increased. Insomuch as the final (downstream) pressure was held fixed at 1591 N/m² (12 mmHg), an increasing pressure head is required to maintain the desired flow rate of 1.67 X 10⁻⁵ m³/s (1 L/min), as both viscosity and hematocrit increase. The magnitude of $\Delta P_{i,f}$ (η) and the slope of the linear regression line relating $\Delta P_{i,f}$ (η) to η were significantly greater, for the more severe (a=A/4) compared to the relatively mild (a=A/2) flow obstructions. As viscosity incrementally increased, $\Delta P_{i,f}$ (η) ranged from [71.94 N/m² (0.54 mmHg) to 110.62 N/m² (0.83 mmHg)] and from [352.36 N/m² (2.66 mmHg) to 496.30 N/m² (3.74 mmHg)], for (a = A/2) and (a = A/4), respectively. With regard to hematocrit, $\Delta P_{i,f}$ (η) tended to increase exponentially, rather than linearly.

Flow-averaged flow-energy loss, $\Delta E_{i,f}$ (η), from the right-hand side of Eq (1b), increased progressively as viscosity (Figure 5A), and hematocrit (Figure 5B), increased. The magnitude of $\Delta E_{i,f}$ (η) and the slope of the linear regression line relating $\Delta E_{i,f}$ (η) to η were 4.0 and 3.5 times greater, respectively, for the (a = A/4) compared to the (a = A/2) flow obstructions. As viscosity increased, $\Delta E_{i,f}$ (η) ranged from [22.46 N/m² (0.17 mmHg) to 52.85 N/m² (0.40 mmHg)] and [94.95 N/m² (0.72 mmHg) to 201.80 N/m² (1.52 mmHg)], for (a = A/2) and (a = A/4), respectively. Moreover, if one normalizes $\Delta E_{i,f}$ (η) to the flow-energy loss associated with the lowest viscosity, i.e. $\Delta E_{i,f}$ (3 X 10⁻³ kg/m-s), the slopes of the regression lines in (Figure 5a) become almost identical, 0.27 and 0.23, for (a = A/2) and a = A/4), respectively. This ratio [$\Delta E_{i,f}$ (η)/ $\Delta E_{i,f}$ (3 X 10⁻³ kg/m-s)] allows focusing on the effect of viscosity by reducing the influence of pathway geometry. This result demonstrates $\Delta E_{i,f}$ (η) depends linearly (directly) on η. With respect to hematocrit, $\Delta E_{i,f}$ (η) increased exponentially, more so for (a = A/4).

II. Flow Expansion (Figure 2B)

Flow-averaged pressure drop, $\Delta P_{i,f}$ (η), increased uniformly as viscosity (Figure 6A), and hematocrit (Figure 6B), increased. The magnitude of $\Delta P_{i,f}$ (η) and the slope of the linear regression line relating $\Delta P_{i,f}$ (η) to η were significantly greater, for the (a = A/4) compared to the (a = A/2) flow obstructions. As viscosity increased, $\Delta P_{i,f}$ (η) ranged from [3.41 N/m² (0.03 mmHg) to 17.36 N/m² (0.13 mmHg)] and from [47.24 N/m² (0.37 mmHg) to 120.98 N/m² (0.91 mmHg)], for (a = A/2) and (a = A/4), respectively. With regard to hematocrit, $\Delta P_{i,f}$ (η) increased exponentially, more so for (a = A/4).

Flow-averaged flow-energy loss, $\Delta E_{i,f}$ (η), increased progressively as viscosity (Figure 7A), and hematocrit (Figure 7B), increased. The magnitude of $\Delta E_{i,f}$ (η) and the slope of the linear regression line relating $\Delta E_{i,f}$ (η) to η were 3.8 and 4.0 times greater, respectively, for the (a = A/4) compared to the (a = A/2) flow obstructions. As viscosity increased, $\Delta E_{i,f}$ (η) ranged from [23.29 N/m² (0.18 mmHg) to 56.45 N/m² (0.43 mmHg)] and [87.73 N/m² (0.66 mmHg) to 221.70 N/m² (1.67 mmHg)], for (a = A/2) and (a = A/4), respectively. Moreover, if one normalizes $E_{i,f}$ (η) to the flow-energy loss associated with the lowest viscosity, i.e. $\Delta E_{i,f}$ (3 X 10⁻³ kg/m-s), the slopes of the regression lines in (Figure 7A) become almost identical, 0.28 and 0.30, for (a = A/2) and (a = A/4), respectively. This result again demonstrates $\Delta E_{i,f}$ (η) depends linearly (directly) on η. With regard to hematocrit, $\Delta E_{i,f}$ (η), like $\Delta P_{i,f}$ (η), increased exponentially, more so for (a = A/4).

Discussion

The Fontan procedure for single-ventricle complex has undergone various modifications aimed at conserving cavopulmonary blood flow's mechanical energy, i.e. pressure energy <P> plus kinetic energy <K>. To this end, de Leval et al.[11], Puga et al.[12] and Pearl et al.[13] devised the Total Cavopulmonary Connection, the combination of a bidirectional Glenn shunt (superior vena cava to the right pulmonary artery) and a conduit from the inferior vena cava to the right pulmonary artery. It was reasoned the Total Cavopulmonary Connection - direct connections from the vena cava to the pulmonary arteries (rather than requiring systemic venous return to pass through the right atrium) - would result in more energy-sparing (streamline) blood flow patterns[6,14-16]. Nevertheless, these patients can develop cavopulmonary obstruction and/or elevated hematocrit, both of which impede pulmonary blood flow.

As a consequence, impaired systemic venous return to the lungs can result in the formation of collateral vessels, in an attempt to: improve systemic arterial oxygenation (systemic arterial to pulmonary arterial connections) and/or bypass systemic venous obstruction (systemic venous to systemic venous and/or systemic venous to atrial/pulmonary venous connections). Systemic venous to systemic venous collateral vessels have minimal effect on systemic arterial saturation, although
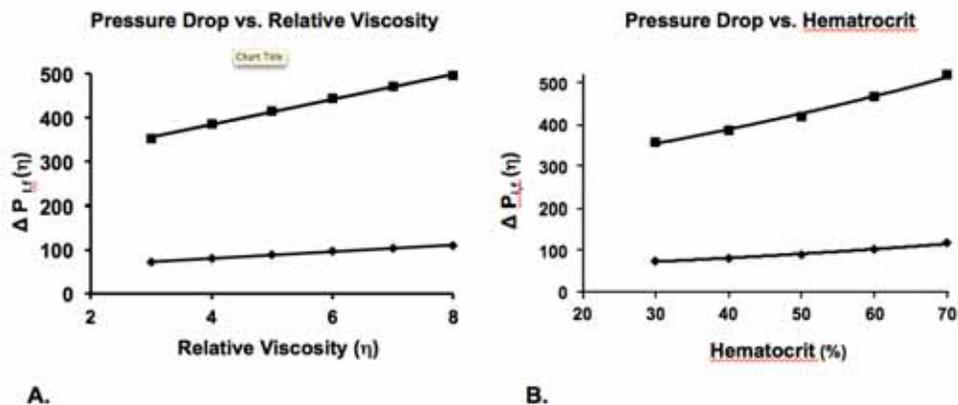
Figure 4: A. *Shows pressure drop $\Delta P_{i,f}$ (η), in N/m^2, on the y-axis and relative viscosity (η), unitless, on the x-axis, for flow contraction. The linear regression lines are $y = 28.70\ x + 269.03$ ($R^2 = 0.99$) for ($a = A/4$) upper graph (■) and $y = 7.72\ x + 49.48$ ($R^2 = 0.99$) for ($a = A/2$) lower graph (♦).*
B. *Shows pressure drop $\Delta P_{i,f}$ (η), in N/m^2, on the y-axis and hematocrit (%) on the x-axis. The exponential regression lines are $y = 267.52\ e^{\ 0.0093x}$ ($R^2 = 0.99$) for ($a = A/4$) upper graph (■) and $y = 51.14\ e^{\ 0.012\ x}$ ($R^2 = 0.99$) for ($a = A/2$) lower graph (♦).*
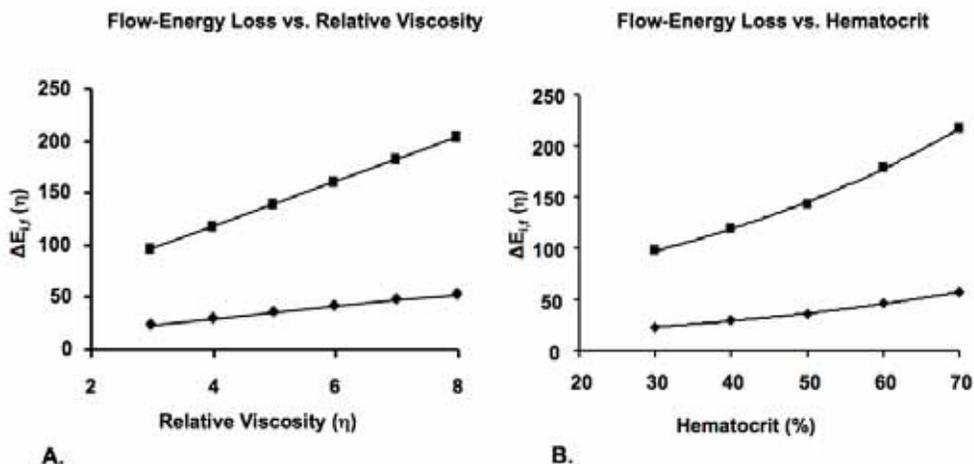

Figure 5: *Flow Contraction - **A.** Shows flow-energy loss $\Delta E_{i,f}$ (η), in N/m^2, on the y-axis and relative viscosity (η), unitless, on the x-axis, for flow contraction. The linear regression lines are $y = 21.35\ x + 31.55$ ($R^2 = 1.0$) for ($a = A/4$) upper graph (■) and $y = 6.07\ x + 4.34$ ($R^2 = 1.0$) for ($a = A/2$) lower graph (♦).*
B. *Shows flow-energy loss $\Delta E_{i,f}$ (η), in N/m^2, on the y-axis and hematocrit (%) on the x-axis. The exponential regression lines are $y = 53.27\ e^{\ 0.02x}$ ($R^2 = 0.99$) for ($a = A/4$) upper graph (■) and $y = 11.74\ e^{\ 0.023x}$ ($R^2 = 0.99$) for ($a = A/2$) lower graph (♦).*

cyanosis from chronic right to left shunting can override the increase in cardiac output, ultimately resulting in poor hemodynamic performance of the Fontan circulation, and significant clinical symptoms in the patient.

Pressure and viscosity are essential defining qualities of a fluid in motion. Whereas pressure provides a driving force for flow, viscous interactions within the fluid create a restraining force against flow. If viscous effects were absent, pressure would remain essentially constant along an unobstructed fluid pathway, gravity not considered. When a fluid is viscous, flow can still be steady. However, a pressure gradient must exist to counterbalance viscous resistance to flow. (In analogy, a voltage drop is needed to overcome the opposition a conductor offers to the passage of a current, as a consequence of energy dissipation.) In contrast, flow becomes non-steady when required to negotiate an abrupt decrease or increase in the caliber of a vessel or conduit. Fluid must suddenly contract and accelerate as it enters and expand and decelerate as it leaves a region of narrowing. The process initially involves conversion of pressure energy into kinetic energy and subsequently kinetic energy back into pressure energy, a reflection of the Bernoulli effect. However, as a fluid speeds up or slows down, pressure and kinetic energy are lost through viscous interactions. Consequently, recovery of mechanical energy is incomplete[7,19]. Thus, a fluid transition associated with energy dissipation gives rise to an increased pressure drop ($\Delta P_{i,f}$) and an additional flow-energy loss ($\Delta E_{i,f}$), that are inter-related through Eqs (1).

An important part of this study was to computationally-assess "flow energetics" associated with a viscous fluid moving through a vessel or conduit undergoing an abrupt decrease or increase in cross-sectional area. Based on numerical solutions to the fluid flow equations, we found:
1) the pressure drop, $\Delta P_{i,f}$ (η), to be greater for transitions involving flow contraction (Figure 2A) compared to equivalent transitions involving flow expansion (Figure 2B); in contrast, flow-energy loss, $\Delta E_{i,f}$ (η), was comparable in magnitude for the inverse processes, and
2) $\Delta P_{i,f}$ (η) and $\Delta E_{i,f}$ (η) to increase linearly (directly) with increasing viscosity (η) and proportionately with severity of obstruction. These findings can be conceptualized by using Eq. 1 in conjunction with a simplified model to describe the flow-energy dissipation.

they do permit cavopulmonary blood flow to bypass the lungs. However, when systemic venous collaterals decompress directly to the pulmonary veins and left atrium (Figure 1), they provide a major source for systemic arterial desaturation. The arterial collaterals tend to increase pulmonary blood flow; whereas, the venous collaterals decrease it. Studies have shown the augmented cardiac output from right to left flow through a fenestration and/or venous collaterals more than offsets the consequent cyanosis, by providing greater peripheral systemic arterial oxygen delivery[17-18]. However, excessive

Equation (1) may be re-written as follows: $\Delta P_{i,f} = \Delta K_{f,i} + \Delta E_{i,f}$, where $\Delta K_{f,i} = (<K>_f - <K>_i)$ represents the overall change in kinetic energy for the fluid transition. For simplicity, we assume flat flow-velocity profiles. In this limit, kinetic energy reduces to $<K> \sim \rho/2\, Q^2/A^2$ or $<K> \sim \rho/2\, Q^2/a^2$, with $A > a$. Based on continuity of flow, for flow contraction ($A \rightarrow a$), $<K>_f$ is greater than $<K>_i$ implying $\Delta K_{f,i} > 0$, an increase in kinetic energy. Conversely, for flow expansion ($a \rightarrow A$), $<K>_f$ is less than $<K>_i$ implying $\Delta_{f,i} < 0$, a decrease in kinetic energy. Hence, if for the fluid reactions considered, flow-energy loss, $\Delta E_{i,f}$, is similar in magnitude for inverse transitions (as shown below), $\Delta P_{i,f}$ becomes greater for flow contraction ($\Delta K_{f,i} + \Delta E_{i,f}$) compared to flow expansion ($-\Delta K_{i,f} + \Delta E_{i,f}$). The larger pressure drop, or greater pressure head, required for flow contraction compared to flow expansion can be further quantified by estimating the difference between the pressure drops for flow contraction [$\Delta P_{i,f}$ ($A \rightarrow a$)] and flow expansion [$\Delta P_{i,f}$ ($a \rightarrow A$)]; namely, [$\Delta P_{i,f}$ ($A \rightarrow a$) - $\Delta P_{i,f}$ ($a \rightarrow A$)], which reduces to $\rho(Q/aA)^2 (A^2 - a^2)$. For the lowest viscosity value considered, $\eta = 3 \times 10^{-3}$ kg/m-s, this difference [….] is positive, namely 68.9 N/m^2 (0.5 mmHg) and 344.8 N/m^2 (2.6 mmHg), for (a = A/2) and (a = A/4), respectively. These differences in pressure drops increase as (η) increases (see Figures. 4 and 6). The results are in qualitative agreement with those obtained using the fluid flow equations.

Since downstream pressure ($<P>_f$) was held fixed, the increase in $\Delta P_{i,f}$ (η) with increasing viscosity reflects the greater pressure head ($<P>_i$) required to maintain a constant flow rate and yet still overcome viscous (shear) forces impairing flow. Pressure drops averaged $\sim$132 N/m^2 ($\sim$1 mmHg) for the various flow transitions considered. We have previously shown, small pressure changes ($\sim$0.5 mmHg) across even mild anatomic obstructions can be associated with significant energy depleting flow disturbances - flow stagnation and flow reversal - in a passively - perfused fluid system, such as a Fontan cavopulmonary pathway[7,19]. Elevated hematocrit (>45%) would worsen such fluid-dynamic derangements in-vivo through its effect on blood viscosity, insomuch as viscosity increases disproportionately with rising red blood cell volume (Figure 3). Conditions that contribute to elevated pulmonary artery pressure and flow-energy loss in a Fontan circuit can have serious clinical manifestations. Cavopulmonary hypertension has been implicated in the development of systemic venous collaterals, pulmonary arteriovenous fistulae[20] and protein-losing enteropathy [21].

Flow-energy dissipation can be conceptualized by considering a model in which the fluid pathway (Figure 2) is composed of two contiguous tubular resistance vessels, one with cross-sectional area (A) and the other with cross-sectional area (a), or vice versa. Assuming steady (Poiseuille) flow, total resistance (R_T) in the circuit becomes $R_T = \eta\, 4\pi\, (L/A^2)\, [1 + (A/a)^2]$, where ($\eta$) is fluid viscosity, (L) overall pathway length and A(a) the larger (smaller) cross-sectional areas. In analogy to a direct current flowing through a resistor, power loss in the fluid system becomes $R_T Q^2$, where Q (the equivalent of current) is flow rate. Power loss may also be written $\Delta E_{i,f}$ (η) Q, with $\Delta E_{i,f}$ (η) = $R_T Q$ represents the energy dissipated (flow-energy loss) per unit of fluid volume.* In agreement with the fluid flow equations, this simplified model predicts $\Delta E_{i,f}$ (η) to be similar in magnitude for inverse processes, since flow is held fixed and the fluid pathway is envisioned as composed of two resistors in series. Since $\Delta E_{i,f}$ (η) is proportional to R_T, it varies linearly (directly) with respect to (η). Moreover, the factor $[1 + (A/a)^2]$ contained in R_T predicts $\Delta E_{i,f}$ (η) to be 17/5 or 3.4 times greater for (a = A/4) compared to corresponding (a = A/2) transitions; the fluid flow equations yield an enhancement factor in $\Delta E_{i,f}$ (η) of $\sim$3.8.

Although the analytical model introduced helps rationalize pressure drops, flow-energy losses and the dependence on fluid viscosity and vessel geometry obtained by numerically solving the Navier-Stokes equations, it underestimates the magnitude of the dissipative effects. As an example, for $\eta = 3 \times 10^{-3}$ kg/m-s, the model accounts for ($\sim$ 17 N/m^2 or $\sim$75%) and ($\sim$59 N/m^2 or $\sim$ 65%) of $\Delta E_{i,f}$ (η), for the (a = A/2) and (a = A/4) fluid transitions, respectively. This underestimate occurs because the model: 1) treats flow as essentially undisturbed in the tubular vessels and 2) does not explicitly account for energy loss arising in the boundary region where flow undergoes the abrupt change in cross-sectional area. As an improvement to this approximation, one might consider including an additional dissipation term that reflects a transitional flow-energy loss arising as a consequence of the sudden difference (A–a) in the pathway cross-sectional area. Using continuity of flow, such a term most likely would be related to the kinetic energy of relative motion between the incoming and outgoing fluid streams, i.e. $\sim\rho/2\, (Q/aA)^2 [A - a]^2$ (See Appendix in Ref. 5). In contrast, the Navier-Stokes equations utilized for our computational analysis provide a comprehensive and quantitative description of a viscous fluid traversing a region of obstruction, by linking pressure and flow-energy to the underlying fluid motion. Unfortunately, for most fluid-dynamic systems, these interrelated differential equations possess no analytical solution. Therefore, numerical analysis is required to obtain accurate results for quantities of clinical interest.

In a passively perfused fluid system, the nature of flow recovery downstream from an obstruction has an important impact on energy wastage. In the case of a decrease in cross-sectional area (A → a), flow accelerates as it enters the narrower portion of the vessel. Here, flow is "pinched" into a smaller area ($a_c < a$), forming the so-called vena-contracta. The size of the vena-contracta depends on the ratio (a/A) and is proportional to the Reynolds number of the incoming flow. For the low Reynolds numbers encountered in the present study, the vena-contracta is less-well developed. Nevertheless, energy can still be lost as fluid disturbances unfold between the stream emerging from the vena-contracta and the vessel wall.

In the case of an increase in cross-sectional area (a → A), flow decelerates as it encounters the more slowly moving fluid in the wider portion of the vessel. Although a fluid can speed up relatively efficiently, it slows down inefficiently and, in doing so, flow-energy is lost. Most of the energy is diffused laterally, as the stream emerging from the obstruction mixes with the surrounding fluid. Moreover, in our model, a considerable distance (>3.5 cm) was required for flow to reach
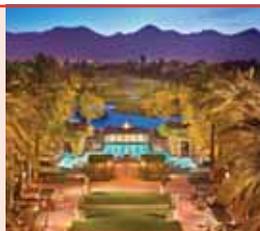
---

*(The reader may recognize from our electrical analogue that $\Delta E_{i,f}$ (η) = $R_T Q$ resembles the voltage drop (ΔV) arising from a current (I) flowing through a resistor (R), as ($\Delta V = R\, I$). The fluid counterpart of this equation ($\Delta P = RQ$) holds for an unobstructed vessel, insomuch as the overall change in kinetic energy of the flow is negligible. However, in general, for a fluid transition, $\Delta P_{i,f}$ (η) has two components:
1) a pressure change associated with the overall change in kinetic energy ($\Delta K_{f,i}$) and
2) a pressure loss arising as a consequence of flow-energy dissipation ($\Delta E_{i,f}$).

Pressure Drop vs. Relative Viscosity
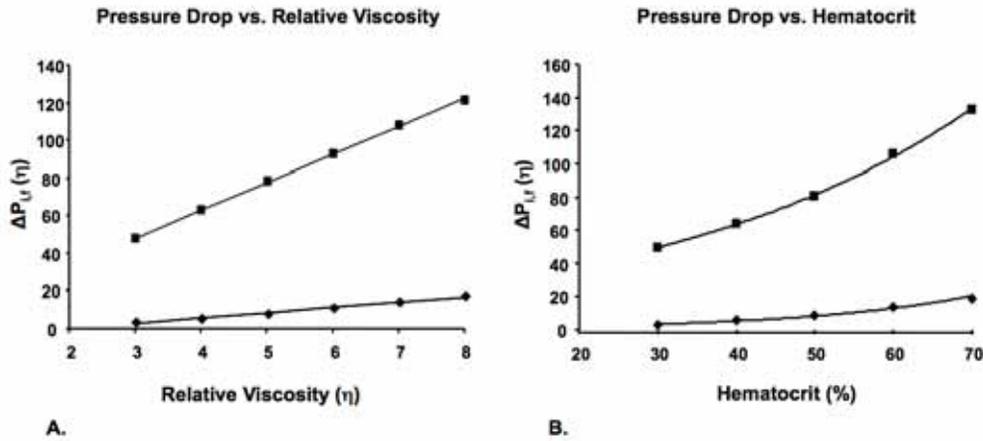
A.

Pressure Drop vs. Hematocrit

B.

Figure 6: - Flow Expansion - A. Shows pressure drop $\Delta P_{i,f}$ (η), in N/m², on the y-axis and relative viscosity (η), unitless, on the x-axis, for flow expansion. The linear regression lines are $y = 14.86 x + 3.12$ ($R^2 = 0.99$) for (a = A/4) upper graph (■) and $y = 2.81 x - 5.72$ ($R^2 = 0.99$) for (a = A/2) lower graph (♦).
B. Shows pressure drop $P_{i,f}$ (η), in N/m², on the y-axis and hematocrit (%) on the x-axis. The exponential regression lines are $y = 23.50 e^{0.048x}$ ($R^2 = 0.99$) for (a = A/4) upper graph (■) and $y = 0.86 e^{0.045} x$ ($R^2 = 0.98$) for (a = A/2) lower graph (♦).

Flow-Energy Loss vs. Relative Viscosity

A.

Flow-Energy Loss vs. Hematocrit

B.
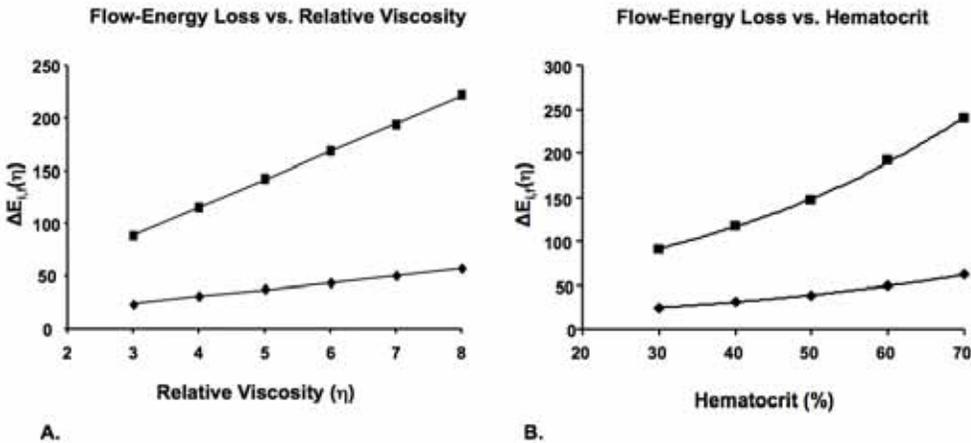
Figure 7: Flow Expansion - A. Shows flow-energy loss $\Delta E_{i,f}$ (η), in N/m², on the y-axis and relative viscosity (η), unitless, on the x-axis, for flow expansion. The linear regression lines are $y = 26.56 x + 8.50$ ($R^2 = 0.99$) for (a = A/4) upper graph (■) and $y = 6.61 x + 3.85$ ($R^2 = 0.99$) for (a = A/2) lower graph (♦).
B. Shows flow-energy loss $\Delta E_{i,f}$ (η), in N/m², on the y-axis and hematocrit (%) on the x-axis. The exponential regression lines are $y = 44.01 e^{0.024x}$ ($R^2 = 0.99$) for (a = A/4) upper graph (■) and $y = 12.15 e^{0.023x}$ ($R^2 = 0.99$) for (a = A/2) lower graph (♦).

equilibration. With Fontan anatomy, the cavopulmonary pathway beyond an obstruction may be of insufficient length to permit flow-velocity profiles to fully develop (recover), which would impair efficient perfusion of the downstream portion of the fluid pathway (see Appendix).

Another factor to consider is the impact an elevated hematocrit may have on pulmonary vascular resistance[22-23]. The relationship between pressure drop across and flow through the pulmonary circulation is complex. Nevertheless, for an isolated, passively-perfused vascular system in which blood flow

is constant, resistance to flow has been shown to increase exponentially with respect to hematocrit[24-25]. In terms of viscosity, the vascular resistance (as we have found) would be expected to increase in a more linear fashion, as viscosity also exhibits a non-linear rise with increasing hematocrit (see Figure 3). In any case, studies suggest that clinical disorders associated with an excessive packed red blood cell volume progressively raise pulmonary artery pressure, through an increase in pulmonary vascular resistance. In Fontan patients, elevated pulmonary artery pressure either from anatomical and/or functional (high hematocrit) obstruction to flow, can promote shunting of blood away from the lungs through rudimentary systemic venous vessels, which ultimately provide auxiliary pathways of lesser resistance. Low velocity and disordered pulmonary blood flow, high hematocrit and hyperviscosity contribute to blood stasis, which in an essentially passively-perfused cavopulmonary system promote thrombus formation.

Lastly, our aim was to study viscosity's effect on flow-energy loss, and to suggest how this may manifest in modified Fontan patients with elevated hematocrits. To this end, we utilized a computational model of fluid through a vessel or conduit undergoing an abrupt decrease (flow contraction) or increase (flow expansion) in a cross-sectional area. The former characterizes viscous dissipation associated with flow entering, and the latter with flow leaving, a region of vessel narrowing. Accordingly, our model was not intended to simulate specific forms of cavopulmonary obstruction. A typical flow rate of 1 L/min was utilized in this study. However, viscous effects can depend on flow rate. Thus, utilizing a range of flow rates to determine viscosity's effect on pressure drop and flow-energy loss would be justified. These calculations are beyond the intent of this paper and await further investigation.

Summary

We studied the influence of fluid viscosity (η) on pressure drop [ΔP (η)] and energy loss [ΔE (η)] associated with non-pulsatile (passive) flow encountering an abrupt decrease or increase in vessel cross-sectional area. Viscosity values reflected clinically- relevant blood hematocrits. The model was designed to simulate blood entering (flow contraction) or leaving (flow expansion) an obstructed portion of a Fontan systemic venous-to pulmonary arterial
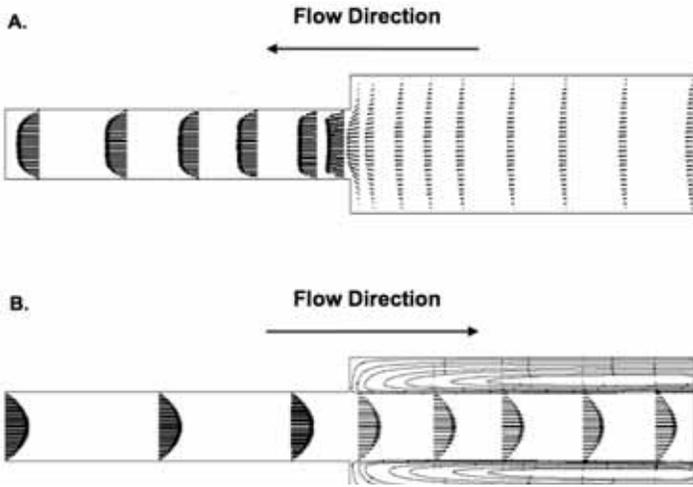
Figure 8: A. Axial velocity profile for flow undergoing an abrupt decrease in vessel cross-sectional area (A →a). As flow contracts to enter the narrower portion of the fluid pathway, it assumes a more rectangular velocity profile, which does not fully recover as flow reaches the outlet of the vessel.
B. Axial velocity profile for flow undergoing an abrupt increase in vessel cross-sectional area (a → A). As flow enters the wider portion of the fluid pathway, it tends to retain its incoming velocity profile, in passing through the more slowly moving surrounding fluid. In doing so, the fluid stream creates a recirculation vortex on the periphery, which extends to the outlet of the vessel, as shown. Calculations were performed for (a = A/4) and with relative viscosity η = 5, a value mid-way between η = 3 − 8.

pathway. Both ΔP (η) and ΔE (η) – determined from numerical solutions to the Navier-Stokes equations – were found to increase significantly with increasing (η) and with severity of obstruction. Our findings have important clinical implications for Fontan patients with elevated hematocrit and with even modest cavopulmonary narrowings. This combination of conditions would contribute to elevated pulmonary artery pressure and promote flow-energy degradation. These factors have been implicated in the failing Total Cavopulmonary Connection, since energy may not be available to maintain adequate blood flow to the lungs and sufficient cardiac output to the body. Based on this work, an important strategy in post-Fontan patients would be to anatomically streamline cavopulmonary passages and to decrease right-to-left shunting of blood through residual defects or venous collaterals, either by interventional catheterization procedures or surgery. We believe maintaining an energy-efficient cavopulmonary blood flow pathway will improve long-term clinical outcome of modified Fontan patients.

Appendix

Energy Balance Equation

In our model, non-pulsatile, incompressible, viscous-fluid flowing through a vessel or conduit was considered to satisfy the overall energy-balance equation [mechanical energy (in - out)/time] :

$$\Delta W_{i,f} = (< P >_i + < K>_i)\, Q_i – (< P >_f + < K >_f)\, Q_f. \quad (1)$$

The quantity $\Delta W_{i,f}$ represents the energy dissipated per time or power loss for the flow transition (i to f). The subscripts (i) and (f) designate the initial (or incoming) and final (or outgoing) portions of the fluid pathway, respectively. Rho (ρ) is the fluid density and Q the flow rate. The terms $< P >$ and $< K >$ represents flow-averaged pressure (P) and flow-averaged kinetic energy (K), respectively, where:

Pressure	$< P > = 1/Q\ \int_A p\,dq$	(2a)
Kinetic Energy	$< K> = 1/Q\ \int_A \rho/2\ v^2\ dq$	(2b)
Flow Rate	$Q =\int_A dq.$	(2c)

Here p and v denote the local pressure (p) and the magnitude of the local velocity (**v**) associated with flow (dq) crossing a differential area (da). The differential flow satisfies $dq = v_N da$, where v_N is the velocity component normal to da. The symbol ($\int$) designates the summation (weighted by the flow) or integration (with respect to the flow) of p and the elemental kinetic energy $\rho/2\ v^2$, as flow is distributed over the conduit's cross-sectional area (A). In general, the fluid-pressure distributions and flow-velocity fields will be dissimilar over the entrance and exit areas, A_i and A_f, respectively. Thus, the corresponding bracketed terms $< >_i$ and $< >_f$, in Eq. (1), which are to be evaluated over A_i and A_f, will take on different values. Equation (2a) reflects the rate pressure force performs work on fluid crossing (A); Eq. (2b) designates the rate kinetic energy is carried by fluid crossing (A). The quantity $\Delta W_{i,f}$ may further be written as $\Delta E_{i,f} Q_f$, or $\Delta E_{i,f} Q_i$ where the flow-energy loss term $\Delta E_{i,f}$ describes the power loss of the fluid system per unit of fluid flow, or the energy loss per unit of fluid volume.

Flow Dynamics

The anatomical obstructions considered in the present study identified important substrates for viscous dissipation, in a passively-perfused fluid system, such as a Fontan cavopulmonary pathway. Pressure gradients and flow-energy losses were found to significantly worsen with increasing viscosity, reflecting underlying energy-depleting fluid-flow disturbances. In the case of a decrease in vessel cross-sectional area (A→a), flow contracts as it enters the narrower portion of the fluid pathway. Continuity of flow demands fluid speed-up (and distribute more equally) across the narrower width of the channel, which results in more-rectangular (non-parabolic) velocity profiles in the contiguous reach. [Compare the more-rectangular velocity profiles for flow leaving the decrease in cross-sectional area (Figure 8A) to the parabolic velocity profiles associated with flow approaching an increase in cross-sectional area (Figure 8B)]. In general, rectangular velocity profiles reflect lower integrated energy of motion (For example, a pure rectangular velocity profile corresponds to a kinetic energy one-half that of a parabolic profile with equivalent flow rate.). For an increase in vessel cross-sectional area (a→A), flow's expansion cannot be accomplished within an infinitesimal distance. Consequently, the more rapidly moving incoming fluid stream tends to retain a parabolic-like velocity profile as it penetrates and passes through the more slowly moving surrounding fluid (Figure 8B). Slower moving peripheral fluid is dragged along by the more rapidly advancing central stream, setting up a large recirculation vortex in the step (the region between the inner and outer radius just distal to the increase in cross-sectional area). This recirculation zone was found to extend fully to the end of the vessel, giving rise to reverse (retrograde) flow along the vessel wall (Figure 8B).

References

1. Thorax. 1971; 26:240-248. Surgical repair of tricuspid atresia. Fontan F. Baudet E.
2. Circulation. 1998; 98:1099-1107. Predictors of early and late-onset supraventricular tachycardia after Fontan operation. Durongpisitkul K, Co-burn JP, Cetta F, Offord KP, Slezak JM, Puga FJ, Schaff HV, Danielson GK, Driscoll DJ.
3. Circulation. 1992; 85:469-496. Five to fifteen-year follow-up after Fontan operation. Driscoll DJ, Offord KP, Feldt R, Schaff HV, Puga FJ, Danielson GK.
4. J Thorac Cardiovasc Surg. 1996; 111:505-513. Use of computational fluid dynamics in the design of surgical procedures: application to the study of competitive flows in cavopulmonary connections. deLeval MR, Dubini G, Migliavacca F, Jalali H, Camporini G, Redington A, Pietrabissa R.
5. Pediatr Cardiol. 2001; 22:110-115. Pressure loss from flow-energy dissipation: relevance to Fontan-type modifications. Ascuitto RJ, Kydon DW, Ross-Ascuitto NT.
6. Pediatr Cardiol. 2003; 24:249-258. Streamlining fluid pathways lessens flow-energy dissipation: relevance to atriocavopulmonary connections. Ascuitto RJ, Kydon DW, Ross-Ascuitto NT.
7. Congenital Cardiology Today (International Edition). 2006; Vol 4, 7:1-11 Energy-depleting fluid-flow disturbances associated with small pressure change: Relevance to obstructed total cavopulmonary connections. Wiesman, JP, Gaver DP, Ross-Ascuitto NT, Ascuitto RJ.
8. Amer. J. Physiol. 1935; 114:128-131. The relation between viscosity of the blood and the relative volume of erythrocytes (hematocrit value). Nygard KK, Wilder M, Berkson J.
9. J Clin Invest. 1962; 41:1591-1598. Influence of flow propertics of blood upon viscosity-hematocrit relationships. Wells RE Jr, Merrill EW.
10. Textbook of Medical Physiology. 6th ed. Philadelphia: W. B. Sanders Co. 1981: Chapter 18, p207. Guyton AC.
11. J Thorac Cardiovasc Surg. 1998; 96:682-695. Total cavopulmonary connection a logical alternative to atriopulmonary connection for complex Fontan operations. Experimental studies and early clinical experience. deLeval MR, Kilner P, Gewillig M, Bull C.
12. 12. Circulation. 1987; 76:III53-III60. Modifications of the Fontan operation applicable to patients with left atrioventricular valve atresia or single atrioventricular valve. Puga FG, Chiavarelli M, Hagler DJ.
13. Ann Thorac Surg. 1991; 52:180-196. Total cavopulmonary anastomosis vs. conventional modified Fontan procedure. Pearl JM, Laks H, Stein DG, Drinkwater DW, George BL, Williams RG.
14. Ann Thorac Surg. 1999; 68:1384-1390. Toward designing the optimal total cavopulmonary connection: An in vitro study. Ensley A, Lych P, Chatzimavroudis GP, Lucas C, Shama S, Yoganathan AP.
15. J Biomech Eng. 2001; 123:317-324. Noninvasive fluid dynamic power loss assessments for total cavopulmonary connections using the viscous dissipation function: A feasibility study. Healy TM, Lucas C, Yoganathan AP.
16. Circulation.1995; 92(9):II322-II326. Comparison by computerized numeric modeling of energy losses in different Fontan connections. Van Haesdonck JM, Mertens L, Sizaire R, Montas G, Purnode B, Daenen W, Crochet M, Gewillig M.
17. Circulation. 1990; Nov;82(5): 1681-1689. Baffle fenestration with subsequent transcatheter closure. Modification of the Fontan operation for patients at increased risk. Bridges ND, Lock JE, Castaneda AR.
18. J Thorac Cardiovasc Surg. 1992; 103:1039-1047. Fenestrated Fontan operation with delayed transcatheter closure of atrial septal defect. Improved results in high-risk patients. Kopf GS, Kleinman CS, Hijazi ZM, Fahey JT, Dewar ML, Hellenbrand WE.
19. Comsol Multiphysics Conference Proceedings. 2005; 411-416. A computational investigation of flow-mechanical energy loss: Relevance to the total cavopulmonary connection. Wiesman JP, Ross-Ascuitto NT, Gaver DP, Ascuitto RJ.
20. Ann Thorac Surg. 2003; Nov;76(5): 1759-1766. Pulmonary arteriovenous malformations after cavopulmonary anastomosis. Duncan BW, Desai S.
21. Congenit Heart Dis. 2007; Sep; 2(5): 288-300. Protein-losing enteropathy after Fontan operation. Rychik J.
22. N Engl J Med. 1982; 306:502-506. Physiologic effects of increasing hemoglobin concentration in left-to-right shunting in infants with ventricular septal defects. Lister G, Hellenbrand WE, Kleinman CS, Talner NS.
23. J Appl Physiol. 1970; 29:866-871. Relative viscosity of blood at varying hematocits in pulmonary circulation. Agarwal JB, Paltoo R, Palmer WH.
24. J Appl Physiol. 1969; 27(3):336-341. Viscosity effects on pressure-flow relations and vascular resistance in dogs' lungs. Murray JF, Karp RB, Nadel JA.
25. The human pulmonary circulation: its form and function in heath and disease. 2nd ed. New York: Churchill Livingstone. 1977:118-136. Harris P, Heath D.

CCT

Corresponding Author

Robert Ascuitto, PhD, MD
Louisiana State University Health Sciences Center
Children's Hospital of New Orleans
Division of Cardiology
200 Henry Clay Ave.
New Orleans, LA, 70118 USA

nrossascuitto @yahoo.com
Phone: (504) 896-9751

Nancy Ross-Ascuitto MD
Department of Pediatrics,
Division of Cardiology
Louisiana State University Health Sciences Center
New Orleans, LA 70112 USA

Children's Hospital of New Orleans
Division of Cardiology
New Orleans, LA, 70118 USA

Martin Guillot, PhD
Department of Mechanical Engineering
University of New Orleans
New Orleans, LA 70148 USA

SCAI View - A Monthly Column: Want to Advance Patient Care? Join SCAI

By Lee Benson, MD

As a pediatric interventional cardiologist, I share your professional interests and goals: to further advocacy, awareness, research and education on behalf of our patients and our profession. One of the most important tools helping me to accomplish these objectives has been my participation in the Society for Cardiovascular Angiography and Interventions. I became a Fellow of the Society in 1994. Since then, SCAI has become a leading advocate for congenital and structural interventionalists worldwide. Through its Congenital Heart Disease and Structural Heart Disease Councils, SCAI has developed a unique infrastructure for fostering cooperation and developing guidelines and standards that lead our specialty into the future. In just the past year, SCAI has taken on several of the most pressing challenges we pediatric interventional cardiologists face, including:

- Supporting the Congenital Heart Futures Act, which seeks to develop federal surveillance programs within the Centers for Disease Control and Prevention for patients with congenital heart disease;
- Publishing a core curriculum for interventional cardiology fellows-in-training who wish to specialize in treating adults with structural and congenital heart disease; and
- Developing performance goals (previously known as objective performance criteria, or OPCs) for stenting the branch pulmonary arteries and other common lesions.

I view my membership as an investment in the development of our field, and I believe as such you, too, will benefit from joining SCAI. The Society provides its members with access to high-quality continuing medical education, opportunities to be an active advocate with federal agencies that directly impact the care we deliver to our patients, and unrivaled options for direct involvement in committees that help set the Society's priorities.

As a member of the Society, you'll also receive a complimentary subscription to *Catheterization and Cardiovascular Interventions* (CCI) featuring the leading research in congenital interventions.

In addition, SCAI offers the extraordinary benefit of community: opportunities throughout the year for pediatric interventional cardiologists to meetings, where we can share knowledge and perspective. In this regard, the breadth of SCAI's educational offerings is substantial. SCAI's Global Interventional Summit brought together the world's leaders in congenital heart disease earlier this fall for a sharing of ideas. Just days ago the SCAI Fall Fellows Courses drew over 50 pediatric interventionalists-in-training for 3 days of training from the leaders in the field. Coming up this May in Baltimore, SCAI 2011 Scientific Sessions is a meeting with an extensive congenital and structural component that will benefit your practice. More importantly, all of these programs are some of the most collegial and intimate venues for networking and brainstorming together to advance patient care.

I urge you to apply for membership in SCAI today. Simply visit the society online at https://www.scai.org/Join. Alternatively, make plans to attend SCAI 2011 at www.scai.org/SCAI2011 and see what SCAI has to offer you and your patients. The Society is still accepting abstracts for this program – presenting authors not only receive complimentary registration but will also have their research published in CCI.

CCT

Lee Benson, MD, FSCAI
Chair, SCAI Congenital Heart Disease Committee
Director, Cardiac Diagnostic and Interventional Unit Cardiology
The Hospital for Sick Children
Toronto, Canada

Review: "Illustrated Field Guide to Adult Congenital Heart Disease"

By James C. Perry, MD

As the authors acknowledge in the preface to the *"Illustrated Field Guide,"* the number of adult congenital heart patients now is greater than those under 18 years of age. This has been the case for more than a decade in the US, making it increasingly likely that these patients will seek care in settings where providers will not have the requisite training or background in adult congenital heart disease (CHD) to recognize and manage the patients' needs. The guidebook from Drs. Lim, Battle and Everett therefore fills
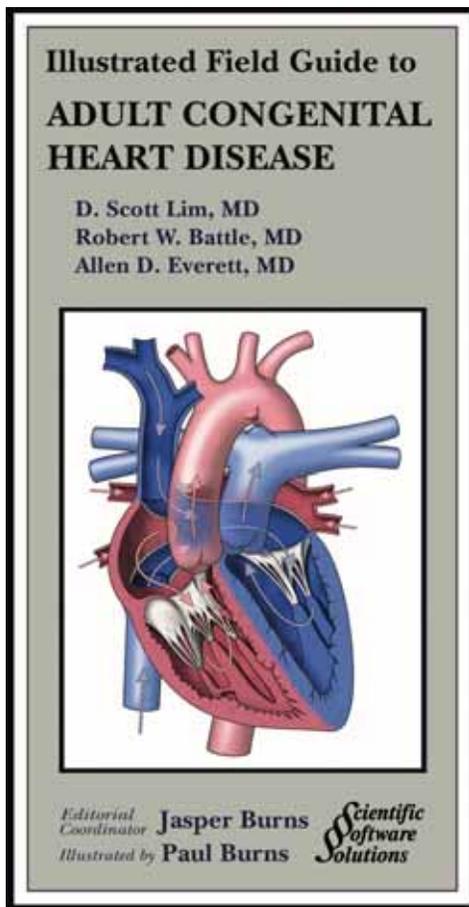
an important niche in medical literature. In recent years, advances have been made in advocacy for the adult CHD population, in attempts to garner health insurance coverage guarantees, reduce the risk of being denied coverage for their "preexisting condition" and increase the chance that research funding will be made available on a national level to understand who these patients are and how do they fare over the long haul. Much of this work has been performed by the

> *"Drs. Lim, Battle and Everett have done an outstanding job putting together a 'rapid resource and reference' for those providers who encounter adult CHD patients in all settings and would like an initial basis of understanding, in preparation for consultation with those trained in adult congenital heart disease management.*

Adult Congenital Heart Association (ACHA) www.achaheart.org in conjunction with professional organizations. Additional efforts are being made to insure that verifiable adult CHD programs exist throughout the US to provide global adult CHD care and importantly, training for future adult CHD cardiologists to care for this growing population. In the meantime, the patients are here already and need wise, coordinated care, often on an urgent basis. The *Field Guide* recognizes that there is a deficit of qualified, trained individuals who are available to see these patients, have the knowledge to care for their current needs, and the ability to anticipate their future needs as well.

The *"Field Guide"* is not intended as a "How To" manual or a substitute for training in managing patients with adult CHD. However, each section of the guide clearly reviews the salient features of each defect:
 (a) anatomy and physiology,
 (b) evaluation,
 (c) medical and surgical management and
 (d) important problems in adult survivors with CHD.

The color illustrations are especially helpful for those with minimal exposure to CHD concepts, including diagrams, echocardiographic snapshots and angiograms. The book is available in a small pocket-size and larger desktop version, has a waterproof cover and a ring binder allowing it to easily lay open for viewing.

The *Field Guide* focuses on the most common CHD lesions the practitioner is likely to encounter, including a section on single ventricle physiology conditions. This section covers Hypoplastic Left Heart Syndrome, tricuspid atresia and other less common CHD lesions. In addition to CHD, the Guide offers sections on adults who had Kawasaki Disease as children (often an overlooked cause of adult angina symptoms), Marfan Syndrome and Eisenmenger Syndrome.

Drs. Lim, Battle and Everett have done an outstanding job putting together a "rapid resource and reference" for those providers who encounter adult CHD patients in all settings and would like an initial basis of understanding, in preparation for consultation with those trained in adult congenital heart disease management. The audience therefore includes trainees, nursing staff, advanced practice nurses, technologists as well as cardiologists. The Guide can serve as a quick reference for pediatric and adult cardiology trainees at the onset of their training in adult CHD. The care of the adult with CHD would benefit from emergency rooms and urgent care providers in particular having on hand a copy of this helpful reference, as well as those who encounter these patients in inpatient settings.

CCT

James C. Perry, MD
Director of Electrophysiology and Adult Congenital Heart Disease Programs
Department of Pediatrics
University of California San Diego
Rady Children's Hospital
3030 Childrens Way, Ste, 201
San Diego, CA 92123 USA
Phone: 858-966-5855
jperry@rchsd.org

Highlights from ISHAC 2010

By Sharon L. Hill, ACNP-BC, PhD(c)

The 5th International Symposium on the Hybrid Approach to Congenital Heart Disease (ISHAC), directed by John P. Cheatham, MD and Mark Galantowicz, MD was held August 31st – September 2nd. There were over 200 participants and faculty from 17 countries and 23 states. ISHAC showcases pioneering work of distinguished faculty who lecture and perform live case demonstrations from the Hybrid Suites at Nationwide Children's Hospital, Rush University Medical Center (Chicago), Miami Children's Hospital, and the University Laboratory Animal Resources Experimental Surgical Suites at The Ohio State University.

This unique meeting began with a hands-on Skills Workshop at the University Laboratory Animal Resources Experimental Surgical Suites (ULAR) at The Ohio State University. The Skills Workshop, led by Ralf Holzer, MD and Alistair Phillips, MD, provided clinicians with one on one experience using Hybrid procedures in animal models in a modern cardiovascular research facility. Individual stations were set up for learning the technical procedures of Hybrid Stage I palliation for HLHS with placement of pulmonary artery bands and pulmonary artery flow restrictors, followed by PDA stent placement; perventricular VSD device closure; & intraoperative stent placement with endoscopic imaging. As in previous Skills Workshops, this hands-on experience, working side-by-side with our experienced, world-renowned faculty provided participants an excellent learning opportunity.

The Skills Workshop was followed by a two day stimulating, interactive symposium with technically challenging case demonstrations from The Rush University Medical Center in Chicago, Miami Children's Hospital, and from the teams at Nationwide Children's Hospital Hybrid Cardiac Catheterization and Operative Suites, as well as from the ULAR suite.

This highly interactive two day symposium presented by international faculty discussed the latest developments and results in Hybrid therapy. The first day of the symposium was dedicated to HLHS. Rick Ohye, MD presented the update of the single ventricle reconstruction trial. Hybrid experiences from abroad were presented by Dietmar Schranz, MD from Germany and the fetal experience from Children's Hospital Boston was presented by Doff McElhinney, MD. Drs. Mark Galantowicz and John P. Cheatham performed a live case demonstration of Hybrid Stage I palliation for HLHS. Stent histopathology, retrograded aortic arch obstruction, and cerebral blood flow in HLHS anatomy was also presented. This culminated with talks on Fontan completion after Comprehensive Stage II, outcomes, VAD assisted Fontan, and transcatheter Fontan completion. A nice overview of the Hybrid approach to RVOT Obstruction, as well as endoscopic guidance in the O.R. for intraoperative stents and exit angiography was provided by Shengshou Hu, MD from China, Alistair Phillips, MD, Evan Zahn, MD,

and Ralf Holzer, MD respectively. This was followed by catheter-based perventricular MVSD closure by Ziyad Hijazi, MD, as well as surgical-based perventricular MVSD closure by Nikolay V. Vasileyev, MD. The live case from Nationwide Children's Hospital Hybrid Operative Suite demonstrating intraoperative bilateral pulmonary artery stenting during pulmonary valve replacement by Drs. Phillips and Holzer created quite a discussion from the audience and faculty.

Day Two of the symposium began with two distinguished Keynote Speakers, Drs. Philip Bonhoeffer and John Byrne. Dr. Bonhoeffer gave a compelling talk on "Having an Idea and Bringing it to Reality…the Melody Experience & Beyond," and was followed by Dr. Byrne addressing "Characteristics of a Successful Hybrid Program." Both left the audience thinking "outside the box." These talks were followed by more exciting talks on new materials and technologies for Hybrid therapies including biodegradable stents, 3-D rotational angiography, MRI imaging, and histotripsy. David Zhao, MD spoke about the "Hybrid Approach in Adult Cardiac Surgery," Ziyad M. Hijazi, MD on "Current Therapy with Aortic Valves," Philipp Bonhoeffer, MD on "Possibilities for Pulmonary Valves," Carlos Ruiz, MD on "Percutaneous Transapical Perivalve Leak Closure using CT Guidance," and Carlos Pedra, MD on "Possibilities in Fetal Cardiac and Pulmonary Interventions." More live cases were also presented culminating in Evan Zahn, MD placing a Melody valve using a perventricular approach at ULAR at The Ohio State University.

Another ISHAC "first" included the presentation of the top three abstracts. The number one abstract "Energy Losses Following Palliative Strategies for Hypoplastic Left Heart Syndrome," a Pilot study using computational fluid dynamics, was presented by Jeffrey Shuhaiber, MD from the Department of Surgery, Cincinnati Children's Hospital, School of Aerospace Systems. Computational fluid dynamics was used to compare the energy loss of the three palliative strategies for HLHS, along with the shear stress at the walls of the heart. Overall energy loss was the highest for the Hybrid procedure in systole compared with Norwoods; however, the shear stress for the hybrid procedure was

After three exciting days, many participants and faculty enjoyed the camaraderie of the opening football game in the "Shoe" at The Ohio State University. The big win at the OSU - Marshall football game was the perfect ending after *ISHAC 2010*!

CCT

lowest among all the palliative strategies for the HLHS. Finally, Hybrid nightmare cases provided insight for thinking "outside the box" when adverse events arise.

An international sports theme for the Gala at The Party Barn on the Wexner estate provided friendly competition at "sporting" events. Participants dressed in their favorite sports team uniform, and showed off any talent they possessed, in shooting basketball, archery, golf, soccer, and even fusball and Nintendo Wii games!

Sharon L. Hill, MSN, ACNP-BC
Interventional Nurse Practitioner
Cardiac Catheterization & Interventional Therapy
The Heart Center
Nationwide Children's Hospital
The Ohio State University College of Nursing
Tel: 614-722-6124 Fax: 614-722-5030

sharon.hill@nationwidechildrens.org

Highlights From Pediatric Cardiology Review 2010

By Anthony C. Chang, MD, MBA, MPH

This popular comprehensive review course of pediatric cardiology, held at the spectacular Ritz-Carlton Resort in Laguna Niguel near Laguna Beach, California, was attended by over 200 attendees from August 29th to September 3rd. While most of the audience was pediatric cardiologists taking either the board or recertification examinations, there were also many attendees from other specialties (pediatric intensive care, adult cardiology, cardiac surgery, neonatology, and nursing) who attended the course as an opportunity to review the entire field of pediatric cardiology in less than one week. The outstanding faculty, which was specially-selected based on their teaching and expertise, was a true "dream team" faculty from some of the top institutions.

Each of the comprehensive morning sessions included didactic lectures covering core cardiology concepts (such as molecular biology of cardiology, pulmonary circulation, cardiac pharmacology, etc), followed by comprehensive review of congenital heart lesions (including embryology, anatomy, physiology, and surgery). The second half of the intense morning sessions included select cardiology topics (such as genetic disorders, systemic diseases, Kawasaki disease, etc) as well as subarea reviews. A fast-paced 15 to 30 minute question and answer period concluded the morning sessions.

There were two special mini-symposia that focused on traditional weak areas in pediatric cardiology fellowships: exercise physiology and electrophysiology. A part of each afternoon was left free for attendees to enjoy the summer weather in Laguna Beach, either by the pool or on the beach. The breaks were welcomed after the intense morning sessions.
The late afternoon sessions included one-hour workshops to emphasize the concepts of the subareas reviewed earlier in the day and a 60-minute board question review session that covered twenty questions per session (with answers explained).

The overwhelmingly positive preliminary reviews by the attendees attest to the high quality of the faculty and the value of this comprehensive pediatric cardiology review course. The next *Pediatric Cardiology Review* will be held in 2012.

CCT

Anthony C. Chang, MD, MBA, MPH
Director, Heart Institute
Children's Hospital of Orange County
455 South Main St.
Orange, CA 92868-3874 USA

AChang@CHOC.org

on behalf of course directors:

Benjamin W. Eidem, MD, FACC, FASE
and
Frank Cetta, MD, FACC, FASE
Mayo Clinic
Rochester, MN USA

Medical News, Products and Information

Doctors Urged to Minimize CT Scans in Children

A CT scan can mean the difference between an accurate and a wrong diagnosis, timely and delayed treatment and, in some cases, life and death. But because CT scans and other tests that use X-ray technology expose the body to often large doses of radiation, their unnecessary, repeated and excessive use may increase cancer risk, especially in children.

Radiologists from Johns Hopkins Children's Center and elsewhere are sounding the alarm and urging judicious use of radiation-based imaging in children. Some 7 million CT scans are performed in children every year in the US, many of them avoidable, the doctors say.

"CT scans save lives and have revolutionized medical diagnostics, but as physicians, we should remind ourselves that every CT scan we order now stays with a child for a lifetime," said pediatric radiologist Melissa Spevak, MD, during a recent presentation at Hopkins, the first of several she is giving to help educate fellow physicians, nurses and radiology technicians about ways to reduce radiation exposure in children. Her efforts are inspired by the "Image Gently" campaign of the Society for Pediatric Radiology and the Alliance for Safety in Pediatric Imaging.

Before ordering a CT scan, Spevak says doctors should ask the following critical questions: "Is this the right test for this condition?" and "Can I obtain the answer in another way?" If the answer to the first question is yes and the answer to the second question is no, the next question should be, "What is the minimum dose that will give me the answer?"

To minimize radiation, doctors suggest the use of alternative imaging technologies like MRI and ultrasound whenever possible, imaging only the indicated body area, avoiding multiple scans, and using the lowest amount of radiation based on the child's size or age.

The safe threshold for radiation exposure has not been defined, but cancer risk is cumulative, rising in proportion to the dose received, with each subsequent exposure increasing that risk, according to a 2005 landmark report by the National Academy of Sciences.

Exactly how likely one is to develop cancer from medical imaging remains the subject of debate, but a 2007 study in the *New England Journal of Medicine* estimated that up to 2% of all cancers in the United States may stem from medical radiation. Epidemiological studies have shown increased cancer among people exposed to nonmedical radiation at doses ranging from 5 to 150 millisieverts (a unit of radiation exposure). The natural environmental radiation people absorb per year is between 3 and 3.5 mSv. An abdominal CT scan in an adult person delivers anywhere between 1 and 30 mSv or up to nine years worth of natural environmental radiation in a single dose. But an abdominal scan in a newborn may result in a much higher dose if the CT scanner settings are not adjusted to the infant's smaller size. By comparison, a set of dental X-rays delivers 0.005 mSv, a chest X-ray delivers 0.01 mSv, and a mammogram delivers around 3 mSv.

MEDICAL MEETING PROGRAM OVERVIEW - JANUARY

Sudden Cardiac Arrest in Children and Adolescents -
Diagnosis, Therapy and Prevention
January 14-15, 2011; Disney Grand Californian, Anaheim, CA USA
www.choc.org/cardiacconference/

Program Director: Anjan S. Batra, MD, Medical Dir. of Electrophysiology at CHOC Children's Heart Institute & Assoc. Prof., Clinical Pediatrics, University of California, Irvine.

Keynote Speaker: Michael J. Ackerman, MD, PhD, Prof. of Medicine, Pediatrics, & Pharmacology at the Mayo Clinic College of Medicine. Dir. of the Long QT Syndrome/Inherited Arrhythmia Clinic & the Sudden Death Genomics Laboratory, Mayo Clinic.

Conference Planning Committee: Michael J. Silka, MD; Kevin Shannon, MD; Anthony C. Chang, MD, MBA, MPH; and Leslie Anne Rabbitt, MPH

Course Faculty: Seshadri Balaji, MD, PhD; Yaniv Bar-Cohen, MD; Anthony C. Chang, MD, MBA, MPH; Dan M. Cooper, MD; Richard A. Friedman, MD, MBA; Ian H. Law, MD; Marc A. Lerner, MD; Ravi Mandapati, MD; Jagat Narula, MD, PhD; James C. Perry, MD; Beth Printz, MD, PhD; Kevin Shannon, MD; and Michael J. Silka, MD

Friday Program: After Opening remarks by Anjan S. Batra, the program will begin with:
- Causes of Sudden Cardiac Arrest (Disease-based Review) moderated by *Jagat Narula*
- Cardiomyopathies: Hypertrophic, Dilated, or Just an Athlete? - *Anthony C. Chang*
- Electrical Abnormalities: Long QT Syndrome and Beyond - *Yaniv Bar-Cohen*
- Other Causes of Sudden Cardiac Arrest (Coronary Artery Abnormalities, Myocarditis, Commotio Cordis) - *Stuart Berger*
- Sudden Cardiac Arrest in Patients with Congenital Heart Disease - *Michael J. Silka*
- Non-Cardiac Arrest - *Dan M. Cooper*
- After enjoying lunch in Downtown Disney, the afternoon will start with Common Symptoms / Rare Consequences (Case Scenarios):
    - Syncope and Atypical Seizures – *Ravi Mandapati*
    - Chest Pain – When to Worry - *Kevin Shannon*
    - Irregular Heart Beats /Palpitations – *Anjan S. Batra*
- There will be a Debate: ECG Screening Should be Mandatory in All School-aged Children - Pro: *Anthony C. Chang*; Con: *Richard A. Friedman*; Moderator: S*eshadri Balaji*
- The day will end with a Panel Discussion moderated by *Anjan S. Batra*

Saturday Program:
- Keynote Speaker, Michael J. Ackerman, will speak on the "State of Pre- and Post-Mortem Genetic Testing for Sudden Death Predisposing Cardiomyopathies and Channelopathies"
- The meeting with continue with Screening for Patients at Risk of SCD with *Michael J. Silka* as moderator with the following topics:
    - Utility of a Sports Pre-Participation Visit - *Yaniv Bar-Cohen*
    - Utility of Echocardiograms and MRIs in Screening - *Beth Printz*
    - ADHD Stimulant Medications and the Risk for Sudden Cardiac Arrest - *Marc A. Lerner*
    - Management of Arrhythmias in Adults with CHD - J*ames C. Perry*
- There will be a Lunch/Debate: Genetic Testing for Evaluation of Patients at Risk for SCD is a Blessing - Pro: *Anjan S. Batra*; Con: *Seshadri Balaji*; Moderator: *Michael J. Ackerman*
- After lunch, the topic will be Secondary Prevention moderated by *Anjan S. Batra*. Topics include:
    - AED Programs in Schools - *Stuart Berger*
    - Evaluation of the Young Patient with Unexplained Cardiac Arrest - *Ian H. Law*
    - Sports Participation in Patients with Known Heart Disease - *Ravi Mandapati*
- There will be a Debate: Patients with ICDs Should be Allowed to Participate in Competitive Sports; Pro: *Ian H. Law*; Con: *Kevin Shannon*; Moderator: *Richard A. Friedman*

The meeting will end with a Panel Discussion and Closing Remarks by *Anjan S. Batra*

TINY HEARTS INSPIRED HYBRID LABS WITH ACCESS FOR BIG TEAMS.

Fixing a heart from birth through adulthood takes big teams working together. So we examined the needs of leading clinicians when designing our hybrid solutions.

The result: our Infinix™-i with 5-axis positioners and low profile detectors, stays out of the way, but right where needed, providing the best possible access to patients. To lead, you must first listen.

medical.toshiba.com

TOSHIBA
Leading Innovation >>>